where $H'_N(Z)$ is of the form

$$H'_N(Z) = \frac{a'_N Z^{-N} + a'_{N-1} Z^{-N+1} + \ldots + a'_1 Z^{-1}}{b_N Z^{-N} + b_{N-1} Z^{-N+1} + \ldots + b_0} \quad (3)$$

Next we extract the term $d_0 Z^{-1}$ from eqn. 3 and write

$$H'_N(Z) = d_0 Z^{-1} H''_N(Z) \quad (4)$$

where $d_0 = a'_1 / b_0$ and

$$H''_N(Z) = \frac{a''_{N-1} Z^{-N+1} + \ldots + 1}{b'_N Z^{-N} + \ldots + 1} \quad (5)$$

Finally we take the inverse of $H''_N(Z)$ and perform the division at the same end:

$$\frac{1}{H''_N(Z)} = 1 + \frac{b''_N Z^{-N} + \ldots + b''_1 Z^{-1}}{a''_{N-1} Z^{-N+1} + \ldots + 1}$$
$$= 1 + Z^{-1} H_{N-1}(Z) \quad (6)$$

Substituting eqns. 4 and 6 into eqn. 2 we arrive at

$$H_N(Z) = c_0 + \frac{d_0 Z^{-1}}{1 + Z^{-1} H_{N-1}(Z)} \quad (7)$$

The realisation of $H_N(Z)$ based on the above expansion is shown in Fig. 1*a*. Repeating the above process, the complete ladder realisation with $2N + 1$ multipliers and $2N$ adders is obtained.

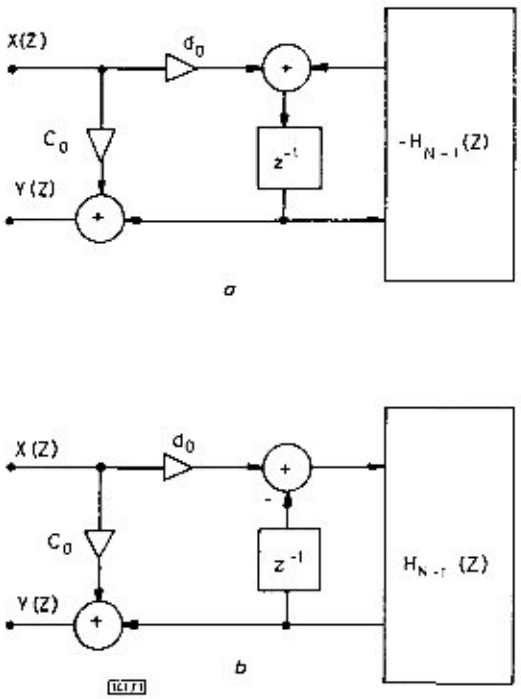

Fig. 1 *Initial steps in the realisation of* $H_N(Z)$
a First method
b Second method

Second realisation method: This realisation is obtained by exchanging the order of the divisions. First we divide out the term $c_0 = a_N / b_N$ for eqn. 1 and write

$$H_N(Z) = c_0 + H'_N(Z) \quad (8)$$

where $H'_N(Z)$ is of the form

$$H'_N(Z) = \frac{a'_{N-1} Z^{-N+1} + \ldots + a'_0}{b_N Z^{-N} + \ldots + b_0} \quad (9)$$

and

$$a'_i = \frac{a_i b_N - a_N b_i}{b_N}, \quad \text{for } i = 0, 1, \ldots, N-1$$

Next we extract the term $d_0 = a'_{N-1}/b_N = (a_{N-1} b_N - a_N b_{N-1})/b_N^2$ and write

$$H'_N(Z) = d_0 H''_N(Z) \quad (10)$$

where

$$H''_N(Z) = \frac{Z^{-N+1} + a''_{N-2} Z^{-N+2} + \ldots + a''_0}{Z^{-N} + b'_{N-1} Z^{-N+1} + \ldots + b'_0} \quad (11)$$

Finally we take the inverse of $H''_N(Z)$ and perform the division at the same end:

$$\frac{1}{H''_N(Z)} = Z^{-1} + \frac{1}{H_{N-1}(Z)} \quad (12)$$

Substituting eqns. 10 and 12 into eqn. 8 we arrive at

$$H_N(Z) = c_0 + \frac{d_0 H_{N-1}(Z)}{1 + Z^{-1} H_{N-1}(Z)} \quad (13)$$

The realisation of $H_N(Z)$ using eqn. 13 is shown in Fig. 1*b*. Repeating the process outlined a complete canonic ladder realisation of $H_N(Z)$ can be obtained containing $2N + 1$ multipliers and $2N$ adders.

Conclusion: The proposed canonic ladder realisations of IIR digital filters preserve all the properties of those suggested by Neuvo and Mitra,[1] and are better than those for realisability. For example, in the first step of realisation we only need for realisability $b_0 \neq 0$ for the first method and $b_N \neq 0$ for the second method.

Acknowledgment: The author wishes to express his sincere thanks to Prof. S. K. Mitra and Prof. Y. Neuvo for helpful discussions.

GONG-TAO YAN* *10th November 1982*

Department of Electronics
China University of Science & Technology
Hefei, Anhwei, People's Republic of China

* The author was with the Department of Electrical & Computer Engineering, University of California, Santa Barbara, CA 93106, USA

Reference

1 NEUVO, Y., and MITRA, S. K.: 'Canonic ladder realizations of digital filters', *Proc. IEEE (Lett.)*, 1982, **70**, pp. 763–764

ENTROPY-CODED HYBRID DIFFERENTIAL PULSE-CODE MODULATION

Indexing terms: Image processing, Differential pulse-code modulation, Fuzzy sets

A hybrid differential pulse-code-modulation (DPCM) system is presented to demonstrate the application of fuzzy set theory in data compression. The system involves entropy coding, Laplacian quantiser and fuzzy enhancement operations as applied on the DPCM signal. Saving of about 0·5 bit is found to be obtained when a DPCM signal is quantised to 32-level, and then Huffman-coded.

Introduction: In image data compression, one is concerned with converting an analogue picture, often generated by optical sensors, to the smallest set of binary integers such that this set of binary digits can be used to reconstruct a replica of the original image. Such a conversion involves removal of redundancy which may arise either by correlation in the data[1]

or by nonuniform probability density[2] of the image data. These two types of redundancies may be removed by differential pulse-code modulation (DPCM) and entropy coding techniques, respectively.

In this letter a hybrid differential pulse-code modulation system (HDPCM) is introduced (Fig. 1) which employs a nonlinear fuzzy transformation $T(d)$[3] (hence the name 'hybrid' is given) on the difference signal before its quantisation. For most pictures the probability density of the difference signal is peaked about zero; the transformation $T(d)$ is chosen so that the differential signal will be more highly peaked about zero.

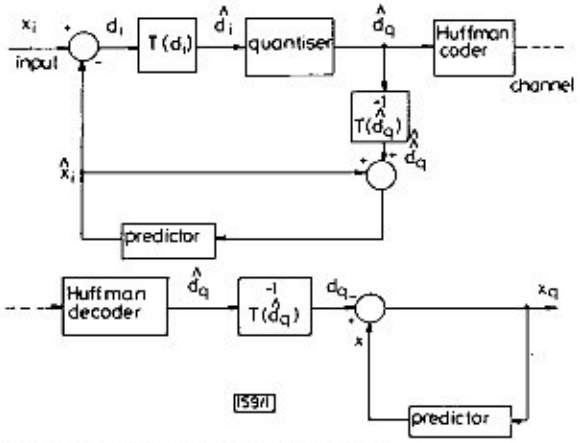

Fig. 1 *Proposed hybrid system (HDPCM)*

This results in a signal with smaller variance which can be transmitted at a lower rate for a given distortion.

The forward and inverse transformations, and the 32-level quantiser are included in the loop in order to use the same predictor at the transmitter and the receiver and also to avoid instability.[1] A Huffman coder is used to encode the quantised difference signal. The effectiveness of this variable bit system is demonstrated on pictures (Figs. 2 and 3) of a man and a telephone box (128 × 128, quantised to 8 bits per pixel), respectively. The different processed versions of the images are presented along with their mean square errors (MSE).

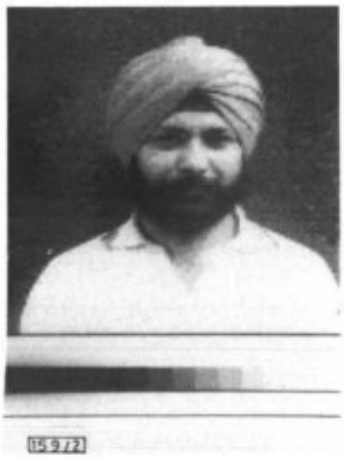

Fig. 2 *Original man picture*

Fig. 3 *Original telephone box*

Hybrid DPCM: The system of Fig. 1 consists of a first-order predictor given by:[1]

(i) Predictor exclusing quantiser and $T(d_i)$:

$$\hat{x}_i = x_{i-1} + (1 - \rho)m \tag{1}$$

$$d_i = x_i - \hat{x}_i \tag{2}$$

where

$i = 1, 2 \ldots (M \times N)$ for an $(M \times N)$ image array x_{mn}

$\hat{x}_i$ = predicted value of x_i

d_i = difference signal

ρ = correlation between adjacent pixels intensity

m = mean grey level of the image

(ii) Transform blocks $T(d_i)$ and $T^{-1}(\hat{d}_q)$:

This block processes the DPCM signal in the fuzzy domain which consists of the following three operations:

(a) transformation from spatial d-domain to fuzzy p-domain ($0 \le p \le 1$) using the standard S function[3]

$$p_i = G(d_i) = 2(|d_i|/d_{max})^2, \quad d_i \le d_{max}/2 \tag{3a}$$

$$= 1 - 2((d_{max} - d_i)/d_{max})^2, \quad d_i > d_{max}/2 \tag{3b}$$

$d_{max}/2$ is the crossover point at which $p_i = 0{\cdot}5$.

(b) enhancing the contrast in the p-domain using the fuzzy intensification operator[4]

$$\hat{p}_i = A(p_i) = 2(p_i)^2, \quad 0 \le p_i \le 0{\cdot}5 \tag{4a}$$

$$= p_i, \quad 0{\cdot}5 < p_i \le 1 \tag{4b}$$

which decreases the values of p_i which are below 0·5 and leaves the rest unchanged. The degree of enhancement can further be increased by making successive use of this A-operator.

(c) inverse transformation $\hat{d}_i = G^{-1}(\hat{p}_i)$ in order to obtain the enhanced spatial domain d_i from the intensified fuzzy p-values.

The block $T^{-1}(\hat{d}_q)$ consists of (a) and (b) above in reverse order.

A uniform 32-level quantiser was used which assumes the signal has a Laplacian distribution. Finally, an entropy code (Huffman code) is used which is very suitable for such a highly peaked distribution.

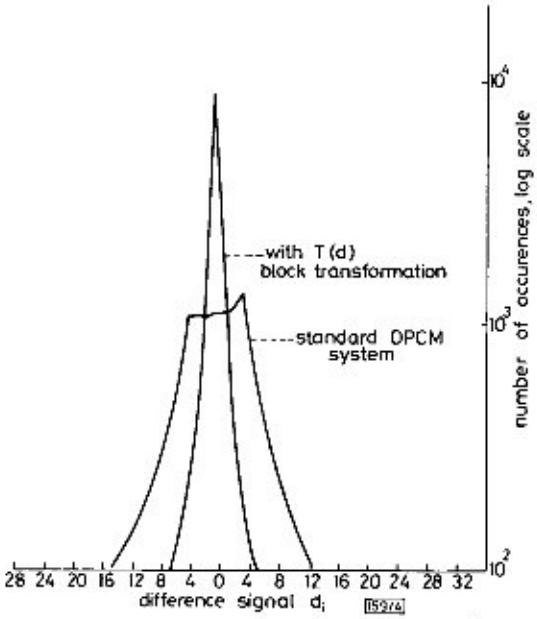

Fig. 4 *Histogram of difference signal with and without transformation $T(d)$*

Implementation and results: The designed system (Fig. 1) was simulated on a digital computer CDC 6400 for two digitised pictures as shown in Figs. 2 and 3. The graph in Fig. 4 gives the histogram of the difference signal d_i before and after transformation for the 'man' picture. From the graph it is seen that after transformation the range of the difference signal becomes much smaller and more highly peaked, and according to entropy theory this can be coded more efficiently by a Huffman coder.[2]

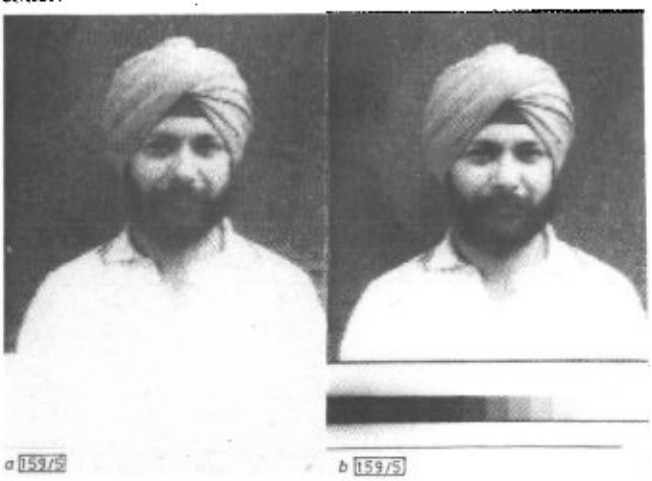

Fig. 5

a Coded to 2·5 bits per pixel, with MSE = $7{\cdot}6 \times 10^{-3}$
b Coded to 3·1 bits per pixel, with MSE $1{\cdot}7 \times 10^{-3}$

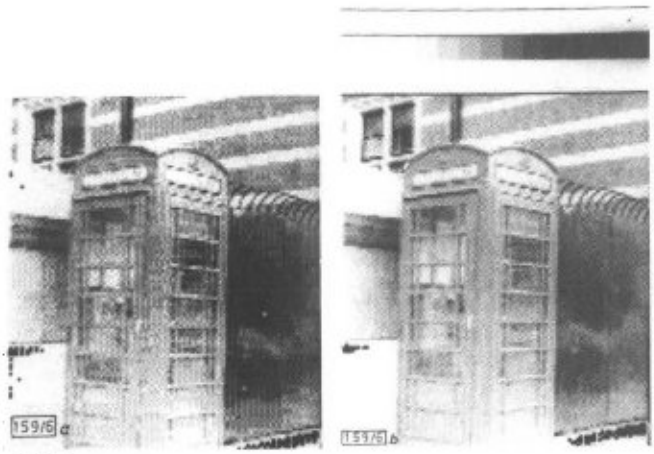

Fig. 6

a Box picture coded to 2·5 bits per pixel, with MSE = $7{\cdot}3 \times 10^{-2}$
b Box picture coded to 3·1 bits per pixel, with MSE = $3{\cdot}6 \times 10^{-3}$

Figs. 5*a* and *b* show the 'man' picture with and without the transformation (block $T(d)$ of Fig. 1) coded to 2·5 bits per pixel and 3·1 bits per pixel, respectively. Figs. 6*a* and *b* demonstrate the coded 'telephone box' under the same processing condition. The corresponding mean-square errors of the processed images are also given. From the above results it appears that the use of a $T(d)$ block can easily save about 0·5 bit with an insignificant degradation over the standard DPCM system.

N. M. NASRABADI
S. K. PAL*
R. A. KING

Electrical Engineering Department
Imperial College of Science & Technology
London SW7 2BT, England

17th November 1982

* On leave from the Electronics & Communication Sciences Unit, Indian Statistical Institute, Calcutta 700 035, India

References

1 GONZALEZ, R. C., and WINTZ, P.: 'Digital image processing' (Addison-Wesley, London, 1977)
2 VIRUPAKSHA, K., and O'NEAL, J. B., JUN.: 'Entropy coded adaptive differential pulse code modulation (DPCM) for speech', *IEEE Trans.*, 1974, **COM-22**, pp. 777–787
3 ZADEH, L. A.: 'Calculus of fuzzy restrictions' *in* 'Fuzzy sets and their applications to cognitive and decision processes' (Academic Press, London, 1975), pp. 1–39
4 PAL, S. K., and KING, R. A.: 'Image enhancement using smoothing with fuzzy sets', *IEEE Trans.*, 1981, **SMC-11**, pp. 494–501

WAVE-THEORETICAL ANALYSIS OF SIGNAL PROPAGATION ON FET ELECTRODES

Indexing terms: Microwave devices and components, MESFETs, Slow-wave phenomena, Waveguide losses

A wave-theoretical analysis of MESFET electrode structures is undertaken, incorporating losses of both the semiconducting layer and the finite conductivity of the electrodes. It is shown that the relevant microwave FET mode has slow-wave properties with a slowing factor of about 6.

Introduction: Several authors[1–3] have analysed the problem of wave propagation along the electrode dimension transverse to electron drift only by a TEM approximation, which is usually questionable since we have a layered structure. A wave-theoretical analysis of a related problem was recently published by Itoh and his coworkers,[4,5] where, however, no relevance to the structure of a FET exists. Therefore the present theoretical results are given here. They are based on a full-wave analysis of the FET structure neglecting active behaviour effects.

The developments of microwave power FETs require, for high output powers with their critical heat-conductance problems, structures of dimensions which are no longer small in comparison to a wavelength. One of the important outstanding theoretical problems in this field is, however, a knowledge of the wavelength on FET structures. Additionally there is a substantial interest in the value of the signal attenuation during propagation along the electrodes, and the origins of this attenuation.

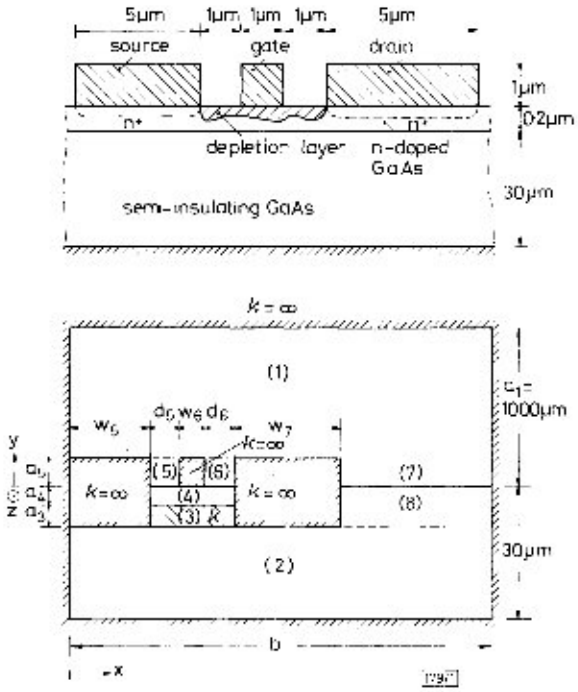

Fig. 1 *Field-effect transistor and its model*

$b = 30\ \mu m$ — $\varepsilon_{r1} = \varepsilon_{r5} = \varepsilon_{r6} = \varepsilon_{r7} = 1$
$w_5 = w_7 = 5\ \mu m$ — $\varepsilon_{r2} = \varepsilon_{r3} = \varepsilon_{r4} = \varepsilon_{r8} = 12{\cdot}9$
$w_6 = d_5 = d_6 = 1\ \mu m$ — $\kappa = 0$ except for region (3)
$a_1 = 1\ \mu m$ — $\mu = \mu_0$ in all regions
$a_3 = a_2 = 0{\cdot}1\ \mu m$